Preparation and Adsorption Selectivity of Rutin Molecularly Imprinted Polymers

Yu Fu,[1,2] Zhenbin Chen,[1,2,3] Hui Yu,[1,2] Yumin Yue,[4] Duolong Di[3]

[1]*State Key Laboratory of Gansu Advanced Non-ferrous Metal Materials, Lanzhou University of Technology, Lanzhou 730050, China*
[2]*School of Material Science and Engineering, Lanzhou University of Technology, Lanzhou 730050, China*
[3]*Key Laboratory for Natural Medicine of Gansu Province, Lanzhou Institute of Chemical Physics, the Chinese Academy of Sciences, Lanzhou 730050, China*
[4]*School of YangJiaQiao, Qilihe District, Lanzhou 730050, China*

Received 18 April 2010; accepted 20 March 2011
DOI 10.1002/app.34525
Published online 9 August 2011 in Wiley Online Library (wileyonlinelibrary.com).

ABSTRACT: Molecularly imprinted polymer (MIP) for Rutin had been prepared through solution polymerization by redox initiation. The effects of monomers, crosslinker, initiators, polymerization time, and temperature on adsorption selectivity for Rutin were investigated and optimized. The structure and surface morphology of MIP were evaluated by Fourier transform infrared spectroscopy and scanning electron microscopy, respectively. The synthesized MIP under the optimal conditions showed a specific recognition of Rutin from the mixture of Rutin and Isorhamnetin. And the maximal separation degree of Rutin was 5.0. © 2011 Wiley Periodicals, Inc. J Appl Polym Sci 123: 903–912, 2012

Key words: synthesis; Rutin; molecular imprinting; copolymer; P(AM-*co*-AA)

INTRODUCTION

Molecular imprinting technology is a novel application technology based on a kind of new polymeric material molecularly imprinted polymer (MIP). Owing to its specific properties, MIP has been applied in many fields, such as separation and analysis, catalysis, antibody and receptor mimics, and sensors,[1] especially in separation and purification. With the successful applications of MIP in separation and purification, researchers have focused their mainly attention on the direct separation of high-value-added active ingredients from Chinese traditional medicine.[2]

Flavonoids, a large class of compounds, exist in nature widely, and most of them possess biological and pharmacological activities, such as antihypertensive, anti-inflammatory, and antiviral.[3–5] Because of the special properties of MIP such as predetermination, specific recognition, and practicability, the separation of high-value-added flavonoids with MIP has been becoming an extensively used method. There are many reports about preparation and application of flavonoids-MIP.[6–10] However, because of the imprinting features of flavonoids-MIP in preparation process, the selectivity of MIP prepared is not ideal. If always study the preparation conditions of high-selective MIP by high-value-added flavonoids, the tremendous economic consume will be unbearable, which would hold back the development of high-selective flavonoids-MIP. The reasonable way is to select a typical and cost-effective flavonoid instead of high-value-added flavonoids to investigate and optimize the preparation conditions.

Rutin is a typical and inexpensive member of flavonoids, because it not only possesses the classical skeleton structure of C_6-C_3-C_6 but also has the residue of hexatomic ring, which are always the basic structure characteristic of flavonoids, and it occupies an important place in the family of flavonoids. The studies of synthesis and selectivity of Rutin-MIP will provide a technical support for the preparation of higher selective MIP using high-value-added flavonoids. However, little report about this aspect can be searched.

In general, selective performance evaluation of MIP is conducted by recognizing template molecule from its nonstructural analog or from a solution only contained template molecule.[11–13] Obviously, the above evaluating methods are unreasonable. This insufficient has been realized, and distinguishing template molecule from enantiomers or similar compounds has been considered.[14,15]

Correspondence to: Z. Chen (zhenbinchen@163.com).
Contract grant sponsor: Lanzhou University of Technology (Doctorial Program Funds); contract grant number: SB01200806.
Contract grant sponsor: Natural Science Foundation of Gansu Province, China; contract grant number: 0809RJZA002.

© 2011 Wiley Periodicals, Inc.

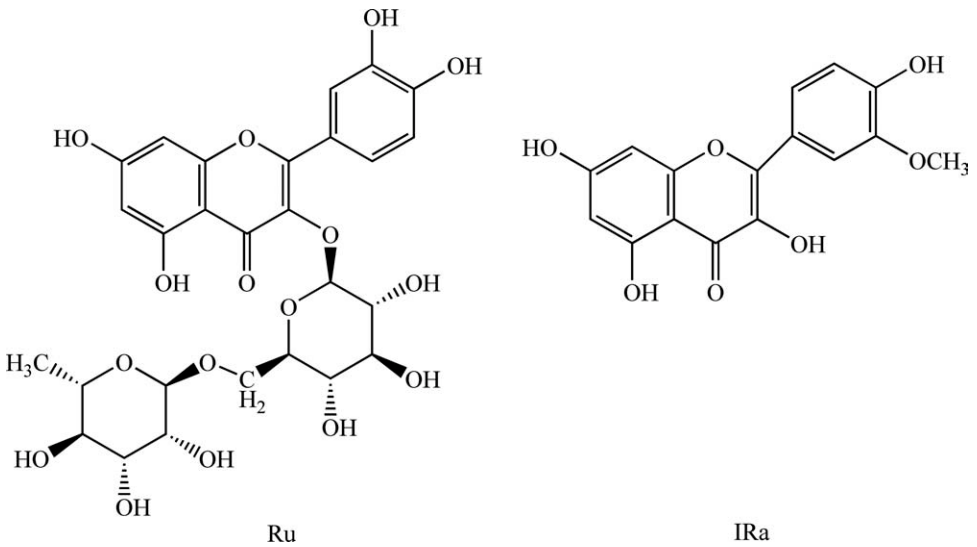

Figure 1 Structural formulas of Ru and IRa.

This work focused on the synthesis of Rutin-MIP with good adsorption performance. To improve the selectivity of MIP, an analog compound, Isorhamnetin, was adopted as interferent, and the adsorption capacity and separation degree were used to characterize the selectivity of MIP during the process of condition optimization. The investigated conditions contained polymerization temperature, reaction time, and each reagent content. The adsorption capacity and separation degree of Rutin-MIP prepared under the optimal conditions were 0.35 mg g^{-1} and 5.0, respectively.

EXPERIMENTAL

Materials

N,*N*′-methylenebiacrylamide (NMBA), L-ascorbic acid (Vc), 30% hydrogen peroxide (H_2O_2) and methanol were obtained from Zhongqin Chemical Reagent Company (Shanghai, China). Acrylamide (AM) was purchased from Kermel Chemical Reagent Company (Tianjin, China). Absolute ethanol was obtained from Yongsheng Fine Chemical Corp. (Tianjin, China). Sodium chloride was purchased from Jianxin Chemical Co. (Shanghai, China). The above reagents were all analytical grade and used as receipted. Acrylic acid (AA, Tianjin Guangfu Fine Chemical Research Institute, China) was purified under reduced pressure to remove the inhibitor before use. Rutin (Ru, Beijing Institute for the Control of Pharmaceutical and Biological Products, China) and Isorhamnetin (IRa, Lanzhou Institute of Chemical Physics, China) were of chromatographic grade. The structural formulas of Ru and IRa were shown in Figure 1.

Determination of maximum absorbance wavelengths

The maximum absorbance wavelength was measured with 752*N* UV–vis spectrophotometer (Shanghai Precision and Scientific Instrument Co., China) by full wavelength scanning method. Ru and IRa were dissolved in methanols of same volume, respectively, and the absorbances of the two solutions obtained were measured in the range of 330–366 nm at intervals of 2 nm against a reagent blank prepared with the same amount of methanol. Figure 2 showed the relationship between absorbance and wavelength. It could be found that the maximum absorbance wavelengths of Ru and IRa solution were 356 nm and 344 nm, respectively.

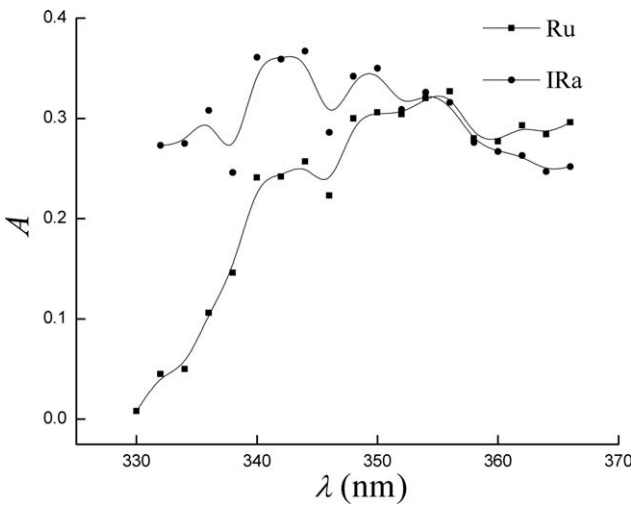

Figure 2 Relationship between absorbances and wavelengths of Ru and IRa. (Scanning range, 330–366 nm; C_{Ru} = 0.0136 g L^{-1}, C_{IRa} = 0.0126 g L^{-1}; T = 298 K; the absorbance at each wavelength was characterized for three times, and the average value was conscripted.)

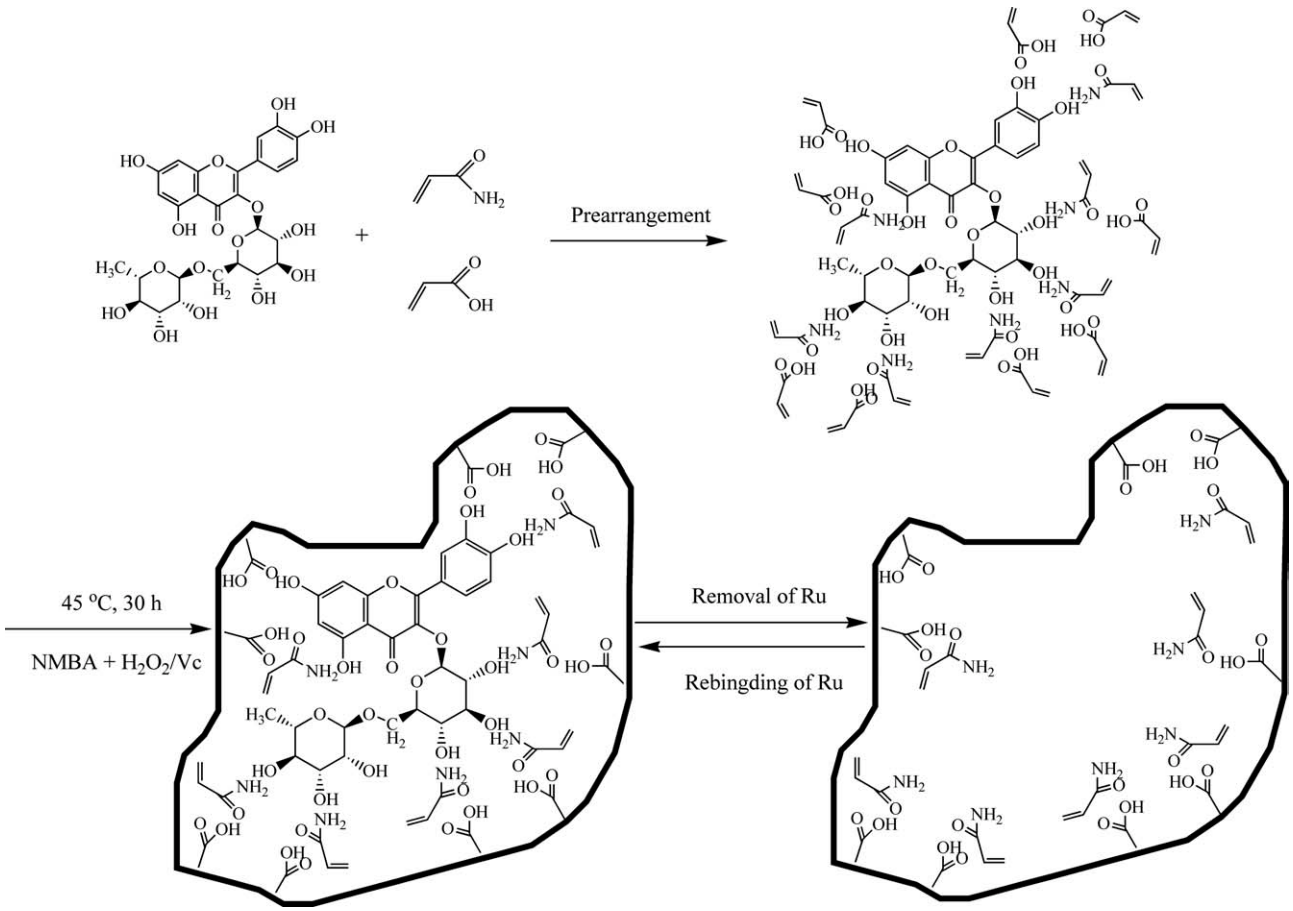

Scheme 1 Schematic representation of the synthesis of MIP for Ru.

Synthesis of MIP

The synthetic reaction was conducted in a 200 mL four-necked flask equipped with a magnetic stirrer, a N_2 line (attached to a bubbler), an addition funnel with a pressure-equalizing side arm, and a thermometer. The flask was kept in 30°C water bath for 15 min. Then, it was charged with 0.5 mL 800 mmol L^{-1} AM ethanol solution, 1.54 mmol L^{-1} Ru ethanol solution, 519 mmol L^{-1} NMBA methanol solution, and AA. The molar ratios of Ru, AA, and NMBA to AM were 0.033, 128, and 35, respectively. After stirred the mixture under nitrogen buffer gas for 10 min, the mixture of 197 mmol L^{-1} H_2O_2 and 56.78 mmol L^{-1} Vc aqueous solution was added, and the molar ratios of H_2O_2 to AM and Vc were 0.074 and 10.3, respectively. After the stirrer stopped, the reaction system was set at 45°C for 30 h. The resultant polymer was dried at 100°C for 8 h and then soaked in 500 mL ultrapure water for 20 h and repeated for six times. After dried, the polymer was ground and extracted by Soxhlet extracted method with ethanol and ultrapure water successively. The process was stopped till the absorbance of extracting solution reached a constant value at each step. Finally, the insoluble polymer was dried and milled through 50–150 mesh screens, and the polymer sustained between the two screens was gathered. Thus, MIP was obtained. Nonimprinted blank polymer (BP) was prepared simultaneously under the same conditions but in the absence of Ru. Schematic representation of the synthesis of MIP for Ru was shown in Scheme 1.

Determination of particle size distribution

Both the range of particle size and the distribution would well affect the characteristics of adsorption, especially the kinetics and dispersion, and so samples with particle size in the range of 50 and 150 meshes were used in tests. The particle size distribution of above sample was determined according to the literature,[16] and the results were as follows: <50 mesh, 0 wt %; 50–80 meshes, 28 wt %; 80–120 meshes, 50 wt %; 120–150 meshes, 21.6 wt %; >150 mesh, <0.4 wt %.

Characterizations of MIP and BP

The structures of MIP and BP were characterized by Fourier transform infrared spectroscopy (FTIR,

Nicolet NEXUS 670, American Nicolet Corp., USA) and scanning electron microscopy (SEM, JSM-5600LV SEM, Japan). The samples used for FTIR characterization were dried completely and ground to fine powder, whereas the samples used for SEM testing were freeze-dried for 15 h after the samples were rinsed to avoid the collapse of porous structures.

Determination of adsorption kinetics

0.5000 g (0.00001, CP225D, Germany Sartorius Co., Germany) of MIP was sealed into a 200-mesh tea bag (2 × 5 cm), the tea bag was submerged into a 100 mL 0.02 g L^{-1} Ru methanol solution at 25°C and then removed at 3 min intervals. The absorbance of raffinate was determined at $\lambda = 356$ nm, and the process was ended after 48 min. Simultaneously, another experiment was carried out as the above testing method, and the reduced volume (V_r), which was caused by the adsorption of MIP, was measured at 3 min intervals. Moreover, an experiment was performed in a baker, which contained 100 mL of methanol, and then the evaporative volume of methanol (V_e) was measured at 3 min intervals. The adsorption capacity (Q) of MIP was calculated according to Eq. (1):

$$Q = \left[C_0 - \frac{C_0 A_{\mathrm{MIP}}}{A_0}\right] \frac{(V_0 - V_r - V_e)}{W} \tag{1}$$

where Q denoted total adsorption capacity of MIP (mg g^{-1}), C_0 represented the concentration of Ru in stock solution (g L^{-1}), A_{MIP} was the absorbance of Ru after MIP absorbing a certain time, A_0 was the absorbance of Ru stock solution, V_0 was the volume of solution before testing (mL), and W was the mass of MIP (g).

Determination of adsorption capacity

0.5000 g of MIP was added into a conical beaker containing 100 mL methanol solution of the mixture of Ru and IRa (the concentration of each component was 0.015 g L^{-1}) for 20 min, then MIP was removed, and the absorbance of the raffinate was measured at 356 nm and 344 nm, respectively. The adsorption capacities of MIP to Ru and IRa were calculated according to following equations:

$$\begin{aligned} Q_e(\mathrm{Ru}) &= (C_0(\mathrm{Ru}) - C_e(\mathrm{Ru}))\frac{V}{W} \\ Q_e(\mathrm{IRa}) &= (C_0(\mathrm{IRa}) - C_e(\mathrm{IRa}))\frac{V}{W} \end{aligned} \tag{2}$$

where Q_e (Ru) and Q_e (IRa) were equilibrium adsorption capacities of Ru and IRa (mg g^{-1}); C_0 (Ru) and C_0 (IRa) presented the concentrations of Ru and IRa in stock mixture (g L^{-1}), respectively; and C_e (Ru) and C_e (IRa) stood for the concentrations of Ru and IRa in raffinate (g L^{-1}) after adsorption equilibrium, respectively; V was the volume of solution tested (mL); W was the mass of MIP (g).

Calculation of separation degree

Separation degree (D) of MIP to Ru and IRa could be calculated by Eq. (3):

$$D = \frac{Q_e(\mathrm{Ru})}{Q_e(\mathrm{IRa})} \tag{3}$$

Characterization of crosslinking density of MIP

The crosslinking density of MIP was measured by swelling degree method: 0.5000 g of MIP (dry weight) was loaded in a 25 mL of volumetric flask, the volumetric flask was filled to mark with 1 mol L^{-1} NaCl solution, which contained in a 25 mL acid burette, and then the residual volume (v_1) in acid burette was recorded. After swelling for 48 h, the solution was removed, and the flask contained swelling MIP was filled to mark as the above method, then the residual volume (v_2) in acid burette was also recorded. The process was repeated for three times, and the average values were conscripted. The swelling ratio (Q^*) was calculated by Eq. (4):

$$Q^* = \frac{v_2 - v_1}{v_1} \tag{4}$$

Thereafter, the crosslinking density of MIP was calculated by Eq. (5):

$$Q^{*5/3} = [(i/2V_u S^{1/2})^2 + (0.5 - \chi_1)/V_1]/(V_e/V_0) \tag{5}$$

where i/V_u was charge concentration of fixing on construction unit (c L^{-1}), S was electrolytic ionic strength of solution, χ_1 was interaction parameter between NaCl solution and MIP, V_1 was specific volume of MIP, and V_e/V_0 was the crosslinking density of MIP. Through above characterization, the crosslinking density of MIP was 75%.

Determination of the average molecular weight

Because MIP was high crosslinked polymer and the average molecular weight could not be determined, the polymer used to determine molecular weight was prepared at the same reaction conditions with that of the optimized MIP except that the crosslinker was not added. 0.2000 g of polymer was loaded in 200 mL of volumetric flask, then 100 mL 1 mol L^{-1}

NaCl solution was added, and the flask was placed into 45°C thermostatic water bath to dissolve the polymer. After the dissolved polymer was transferred to a 25°C ± 0.05°C thermostatic water bath for 30 min, the solution was brought to 200 mL by 1 mol L^{-1} NaCl solution, and the stock solution was obtained. Solutions with different precise concentrations of polymer were prepared by pipetting 20, 15, 10, 5, 2.5, and 1.25 mL of the above stock solution into 25 mL volumetric flask, bringing them to volume by 1 mol L^{-1} NaCl solution, and then placing them in 25°C ± 0.05°C water bath for use, respectively. This process was repeated for three times, and the average values were conscripted. After plotting the relationship curves of reduced viscosity and inherent viscosity with concentration, respectively, the intrinsic viscosity [η] of polymer was obtained. Thereafter, the average molecular weight of polymer was calculated by Eq. (6)[17]:

$$[\eta] = 9.25 \times 10^{-4} M^{0.9} \quad (6)$$

where M was average molecular weight. After determination, M of polymer was 2.6×10^5.

RESULTS AND DISCUSSION

Establishment of concentration measuring method

To calculate the adsorption capacity and the separation degree, the concentrations of Ru and IRa needed to be measured. Figure 2 showed the relationship between absorbances and wavelengths of Ru and IRa. It could be found that Ru and IRa had higher absorbance, which indicated that the concentrations of Ru and IRa could be determined by UV–vis spectrophotometer and had been reported in literature.[9] On the other hand, because Ru and IRa had comparatively large absorbance in each other's maximum absorbance wavelength, they would interfere mutually in the determination of concentration, and the concentrations of Ru and IRa in mixture could not be calculated only by measuring absorbance at the maximum absorbance wavelength of themselves, respectively. Besides, the absorbances of Ru and IRa in all wavelength range were higher, the concentrations before and after adsorption could not be measured by secondary single-wavelength method. To cover the shortages of the maximum absorbance wavelength and secondary single-wavelength method in the determination of concentration, double-peak dual-wavelength method, which focused on the similar problem with the above case, had been presented in literature.[18] In this work, the concentrations were planned to be measured using double-peak dual-wavelength method.

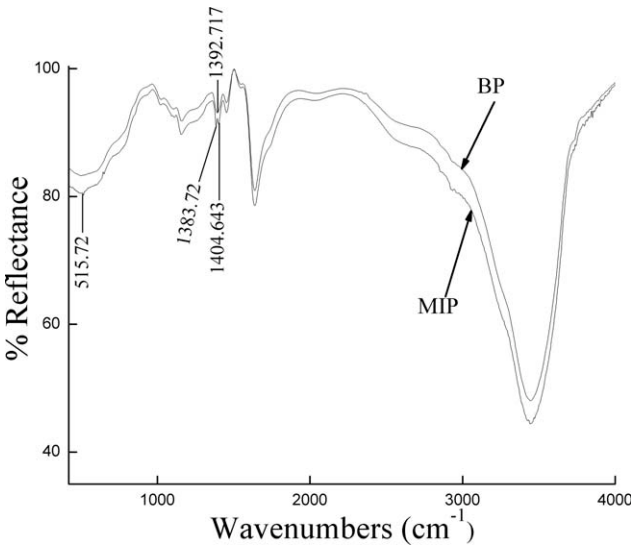

Figure 3 FTIR spectra of MIP and BP.

To prove the feasibility of the above method, the standard curves of Ru, IRa, and the mixture of Ru and IRa ($m_{Ru} = m_{IRa}$ in mixture) were plotted at 344 nm and 356 nm, respectively. The results showed a well linear relationship between absorbance and concentration in the range of 0.018 g L^{-1} – 0.040 g L^{-1} for all solutions of Ru, IRa, and the mixture of Ru and IRa, the regression equations were $A = 11.712C + 0.0201$ ($R^2 = 0.9999$), $A = 13.28C + 0.0782$ ($R^2 = 0.9997$), and $A = 11.545C + 0.0822$ ($R^2 = 0.9992$) at λ = 356 nm; and $A = 10.136C + 0.0154$ ($R^2 = 0.9996$), $A = 13.455C + 0.0968$ ($R^2 = 0.9999$), and $A = 11.917C + 0.067$ ($R^2 = 0.9999$) at λ = 344 nm for Ru, IRa, and the mixture of Ru and IRa, respectively (where A was the absorbance of solution and C was the total concentration of solution). Moreover, the absorbance of mixture was equal to the summation of the absorbances of pure Ru and pure IRa solution with the same concentration. This indicated that there was no any other effect after they were mixed, and the absorbance of the mixture possessed additive property. Thus, the concentrations of Ru and IRa in mixture could be calculated accurately by the double-peak dual-wavelength method, and the system of linear equations was:

$$\begin{cases} A_{356} = 15.00 \times C_1 + 14.58 \times C_2 \\ A_{344} = 12.25 \times C_1 + 15.92 \times C_2 \end{cases}$$

where A_{356} and A_{344} were the absorbances of mixture at λ = 356 nm and 344 nm, and C_1 and C_2 stood for the concentration of Ru and IRa in mixture, respectively.

Characterizations of MIP and BP

Figure 3 showed the FTIR spectra of MIP and BP. It could be found that the FTIR spectrum of MIP was

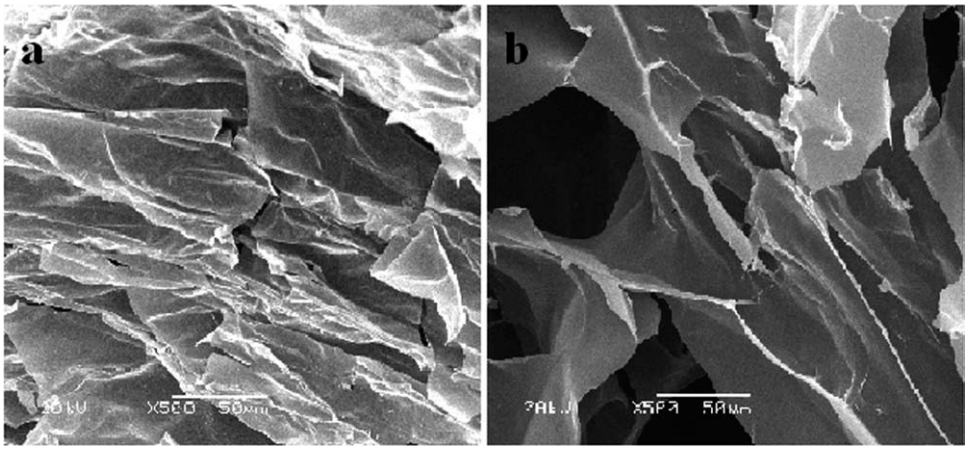

Figure 4 SEM of BP and MIP. (a) BP and (b) MIP.

similar with that of BP. The main peaks of the two spectra were coincident, except that the single peak of BP at about 1393 cm^{-1} split into asymmetric double peaks in MIP at about 1384 and 1405 cm^{-1} as well as the spectrum of MIP appeared a small weak peak at about 516 cm^{-1}. Given that the chemical bonds and the functional groups of BP and MIP are almost identical, the similarity of the two spectra could be understood. The slight differences between MIP and BP might be attributed to the synergy produced by binding sites of imprinting cavities. The results indicated that the structure of MIP would not be effectively characterized only by FTIR.

To characterize the structure of MIP effectively, SEM was adopted to observe the surface morphologies of MIP and BP, and the results were shown in Figure 4. Compared to BP, MIP had rougher surface and more cavities with homogeneous aperture. The results indicated that MIP produced imprinting cavities of Ru.

Adsorption kinetics of MIP

The relationship between Q and adsorption time (t^*) was shown in Figure 5. It could be found that Q increased with increasing t^* and reached maximum after 15 min. At the beginning of adsorption, the unoccupied imprinting cavities in MIP would adsorb Ru to decrease the surplus bonding energy, that is, Ru would be rapidly adsorbed onto imprinting cavities in the shallow layer, and the adsorption speed was high. Thus, Q increased. With the increase of t^*, Ru would enter into the deep layer to find imprinting sites, and the adsorption rate would slow because of the stronger resistance of Ru. Moreover, the adsorption of MIP to Ru was physical process, which was in accordance with the physical process of self-assembly. Thus, with the adsorption degree increased, the desorption rate increased correspondingly. Owing to above two reasons, the adsorption rate decreased. As the desorption rate increased to equal to the adsorption rate, Q would reach maximum and keep as a constant.

Influence of n_{Ru}/n_{AM} on adsorption performance of MIP

The influence of n_{Ru}/n_{AM} on Q and D was shown in Figure 6. It could be found that Q_{Ru} and D rise till $n_{Ru}/n_{AM} = 0.033$ and then continuously deceased, while Q_{IRa} increased first and then slightly decreased. As n_{Ru}/n_{AM} was low, the functional monomers would not take part in the self-assembly process completely, which led to some surplus AM after self-assembly. After polymerization, the surplus monomers would form some arbitrary distributional acting loci; due to the higher hydrophilic of acylamino, large amount of pores formed by the evaporation of solvent would collapse during the drying process[19]; thus, the inner imprinting cavities and acting loci would not join in the adsorption; thus,

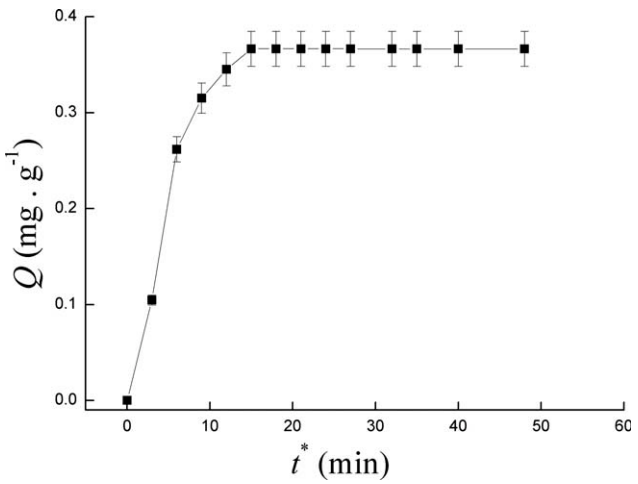

Figure 5 Relationship between Q and t^* ($m_{MIP} = 0.5$ g; $C_{Ru} = 0.02$ g L^{-1}; $T = 298$ K.)

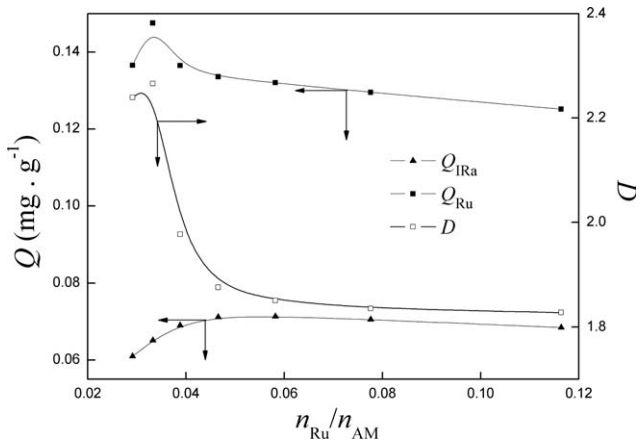

Figure 6 Influence of n_{Ru}/n_{AM} on adsorption performance of MIP (n_{Ru} = 0.013 mmol; n_{NMBA} = 12.6 mmol; n_{AA} = 29 mmol; $n_{H_2O_2}$ = 0.008 mmol; n_{Vc} = 0.002 mmol;$V_{H_2O_2}$ = V_{Vc}; T = 60°C; t = 24 h.

Q_{Ru}, Q_{IRa}, and D were low. With the increase of n_{Ru}/n_{AM}, the surplus amount of AM decreased, and the arbitrary distributional acting loci decreased, which would be favorable to the completeness of imprinting cavities and the adsorption of inner cavities; thus, the relative quantities of effective binding sites increased, and Q_{Ru} and D increased correspondingly. Because of the adsorption of inner acting loci and cavities as well as the similar structure between Ru and IRa, Q_{IRa} increased correspondingly. However, with the excessive increase of n_{Ru}/n_{AM}, the low amount of AM could not reach the necessary amount that assembling with Ru, which would lead to incomplete self-assembly complex. Because of the competitive self-assembly of Ru to AM, the coordination number of AM decreased; thus, more AM tended to distribute arbitrary[20] and then the collapse of pores increased and the imprinting cavities decreased; as a result, the quantities of binding sites decreased, and Q_{Ru}, Q_{IRa}, and D decreased.

Influence of $n_{H_2O_2}/n_{AM}$ on adsorption performance of MIP

Figure 7 showed the influence of $n_{H_2O_2}/n_{AM}$ on Q and D. It could be found that Q_{Ru} and D remained unchanged first with increasing $n_{H_2O_2}/n_{AM}$ till $n_{H_2O_2}/n_{AM}$ = 0.064, then the curves increased and decreased after $n_{H_2O_2}/n_{AM}$ > 0.074, while Q_{IRa} remained basically unchanged with increasing $n_{H_2O_2}/n_{AM}$. As lower initiator was used, due to the consumption of radical by chain transfer and chain termination reactions, certain amounts of the functional monomers and oligomers could not react, which would lead to the incomplete reaction; thus, the average molecular weight was low and soluble polymers increased; after extraction, the imprinting

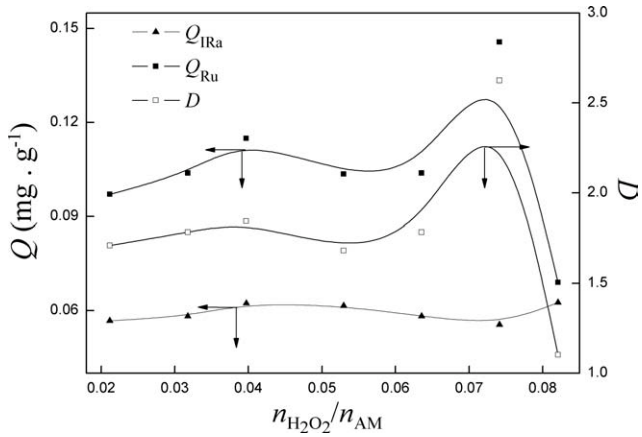

Figure 7 Influence of $n_{H_2O_2}/n_{AM}$ on adsorption performance of MIP (n_{AM} = 0.4 mmol; other conditions were the same as Fig. 6 but $n_{H_2O_2}$ and n_{Vc}).

cavities would deform; thus, Q_{Ru} and D were low. With the increase of initiator, the polymerization speed increased, the amount of soluble polymers decreased correspondingly, and the completeness of imprinting cavities increased, Q_{Ru} and D increased too. However, with the further increase of $n_{H_2O_2}/n_{AM}$, the excessive using of initiator would lead to the fast speed of polymerization, which easily produced the phenomenon of explosive polymerization and increased soluble polymer content. The excessive production of soluble polymer would decrease the completeness of cavities after the extraction process; thereafter, Q_{Ru} and D decreased.

Influence of n_{NMBA}/n_{AM} on adsorption performance of MIP

Figure 8 showed the influence of n_{NMBA}/n_{AM} on Q and D. It could be observed that the larger n_{NMBA}/n_{Ru} was, the higher Q_{Ru} and D were. Because, increasing the amount of NMBA could decrease the

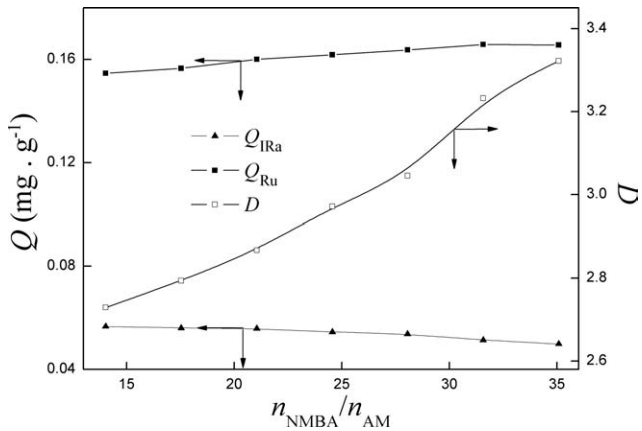

Figure 8 Influence of n_{NMBA}/n_{AM} on adsorption performance of MIP ($n_{H_2O_2}$ = 0.027 mmol; n_{Vc} = 0.008 mmol; other conditions were the same as Fig. 7 but n_{NMBA}).

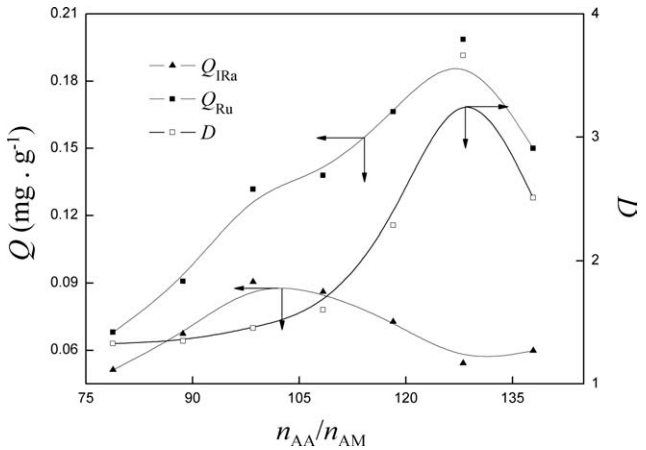

Figure 9 Influence of n_{AA}/n_{AM} on adsorption performance of MIP (n_{NMBA} = 14 mmol; other conditions were the same as Fig. 8 but n_{AA}).

swelling of polymer in solvent and increase the stability of recognition sites, selectivity, and the ability to distinguish structure analogous substances.[21] However, within the scope of experiment, the decrease of Q_{Ru} and D had not been observed, which suggested that the amount of NMBA had not reached the optimum amount[21] because of the limited solubility of NMBA in methanol at lower temperature. From the figure, it could also be found that Q_{IRa} slightly decreased as increasing NMBA. This verified the increase of NMBA could increase the selectivity of MIP.

Influence of n_{AA}/n_{AM} on adsorption performance of MIP

Figure 9 showed the influence of n_{AA}/n_{AM} on Q and D. It could be found that Q_{Ru}, Q_{IRa}, and D increased first and then decreased with increasing n_{AA}/n_{AM}, while the maximum of Q_{Ru} corresponding to n_{AA}/n_{AM} was higher than that of Q_{IRa}, the ratio that made better Q and D appeared at 128. When n_{AA}/n_{AM} was low, the relative low AA could not effectively arrange with Ru and produce complete self-assembly complex. So, less binding sites existed in the formed MIP, and the shape of imprinting cavities was incomplete, affecting the formation of optimal MIP,[22] and Q_{Ru}, Q_{IRa}, and D were low. With the increase of n_{AA}/n_{AM}, the amount of AA arranged with Ru increased, and the imprinting cavities became complete gradually, then the quantities of binding sites increased, and thus Q_{Ru} and D increased. Although AA increased gradually, the self-assembly between functional monomers and Ru was still incomplete; thus, Q_{IRa} increased. With the further increase of n_{AA}/n_{AM}, the self-assembly between functional monomers and Ru would reach optimum state, and the matching degree between binding sites and Ru was the best; thereafter, Q_{Ru} and D increased, while Q_{IRa} decreased. However, with the excessive increase of n_{AA}/n_{AM}, the amount of AA would become surplus, and these surplus monomers would form some arbitrary distributional acting loci, due to the higher hydrophilic of carboxyl, some pores would collapse during the drying process; thus, the inner imprinting cavities and acting loci would not join in the adsorption, and, thereafter, Q_{Ru}, Q_{IRa}, and D decreased.

Influence of polymerization time on adsorption performance of MIP

Figure 10 showed Q and D obtained from different MIPs, which were prepared with different polymerization times (t), and Q and D appeared maximum values when t was equal to 32 h. In fact, two kinds of polymerization reaction would take place during the preparation of MIP, that is, chain polymerization and stepwise polymerization. The stepwise polymerization mainly took place between —COOH and —$CONH_2$, which would produce imides.[23] Different from the chain polymerization used for preparing MIP, stepwise polymerization was unwanted, because it could form novel crosslinked bond. Because of much slower polymerization rate and higher reaction energy than those of chain polymerization, stepwise polymerization was seriously dependant on time and temperature. So, the influence of polymerization time on Q and D could be explained easily. At the beginning, both polymerization and crosslinking of chain reaction were not completed; thus, Q_{Ru}, Q_{IRa}, and D were low. However, the situation would be improved with increasing t, and the complete imprinting cavities formed correspondingly. Although stepwise polymerization also happened during this time, the reaction degree was much lower than that of chain polymerization.

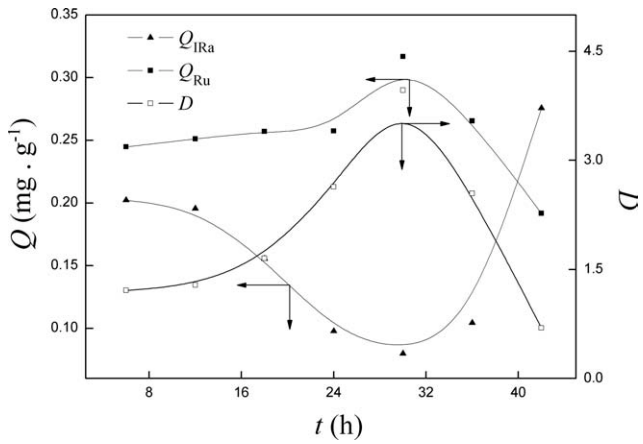

Figure 10 Influence of polymerization time on adsorption performance of MIP (n_{AA} = 51.2 mmol; other conditions were the same as Fig. 9 but t).

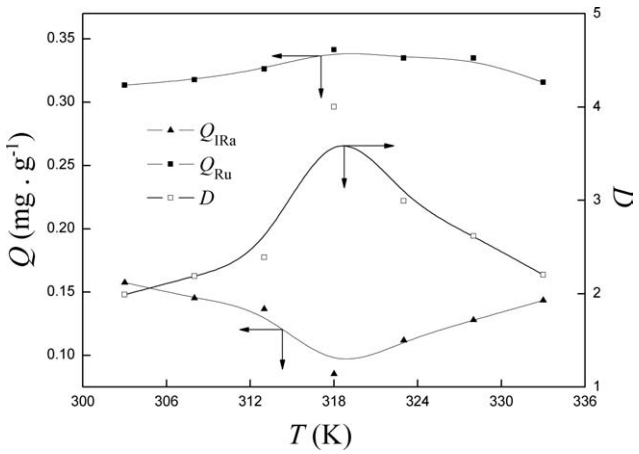

Figure 11 Influence of polymerization temperature on adsorption performance of MIP (t = 30 h; other conditions were the same as Fig. 10 but T).

As a result, Q_{Ru} and D increased to maximum, while Q_{IRa} decreased to minimum. With t further increased, stepwise polymerization would be dominant. Simultaneously, polymerization temperature was relatively high (60°C) in this section; all these would facilitate Ru to escape from the preassembly system and produce some "naked" —$CONH_2$.[23] These "naked" —$CONH_2$ would react with —COOH at the subjacent place to form novel crosslinked bond and to destroy the earlier existed imprinting cavities. These imprinting cavities of Ru in MIP would reduce during the extraction and drying process, which would be disadvantageous to the selectivity of MIP to Ru; thus, Q_{Ru} and D decreased. However, because of the smaller structure of IRa, it was so similar to the residues of Ru, and the cut-down pores formed by the reaction between acid and amide would benefit to the entry into pores of IRa; thus, Q_{IRa} increased.

Influence of temperature on adsorption performance of MIP

Figure 11 showed the influence of temperature (T) on Q and D. Q_{Ru} and D increased with increasing T till T = 45°C and then they decreased. Although Q_{IRa} displayed contradictory trend. Usually, the relative low T would stabilize the template-functional monomers complexes,[24] and low T was favorable to the preparation of MIP based on electrostatic interaction.[25] Thus, Q_{Ru} and D were relatively high. But when T was too low, the degree of polymerization and crosslinking were low, which would increase the amount of soluble polymer. And the completeness of cavities would decrease during the extraction process of soluble polymer; thus, Q_{Ru} and D were low. When T excessive increased, the molecular activity increased, but the bonding of template-functional monomers decreased, that is, the affinity and the formation of binding sites decreased.[26] At the same time, imides formed by the interaction between —$CONH_2$ and —COOH would increase. Therefore, Q_{Ru} and D decreased.

Q_{IRa}, exhibiting the lowest value at 45°C, was because the stronger electrostatic interactions formed more binding sites being available for Ru at 45°C, and this ensured the preferred selectivity of MIP to Ru.

Influence of $n_{H_2O_2}/n_{Vc}$ on adsorption performance of MIP

The influence of $n_{H_2O_2}/n_{Vc}$ on Q and D was shown in Figure 12. It could be found that the variation trends of Q_{Ru} and D were the same, and the maximum values of Q_{Ru} and D could be observed at $n_{H_2O_2}/n_{Vc}$ = 10.3. However, the curve of Q_{IRa} remained basically unchanged. The structure of Vc played an important role in this aspect. When the amount of Vc was high, the similar groups —C=O and —OH of Vc with Ru would compete the functional monomers with Ru in the polymerization process, which would lead to incomplete imprinting cavities; thus, Q_{Ru} and D were low. The influence of surplus Vc on the integrity of imprinting cavities would gradually decrease with increasing $n_{H_2O_2}/n_{Vc}$ because of the decrease of Vc, and Q_{Ru} and D increased accordingly. With $n_{H_2O_2}/n_{Vc}$ further increased, the well synergy between initiators would be destroyed, which decreased the amounts of efficient initiators; thus, Q_{Ru} and D decreased.

CONCLUSIONS

A novel molecularly imprinted polymer was prepared by solution polymerization of AM and acrylic

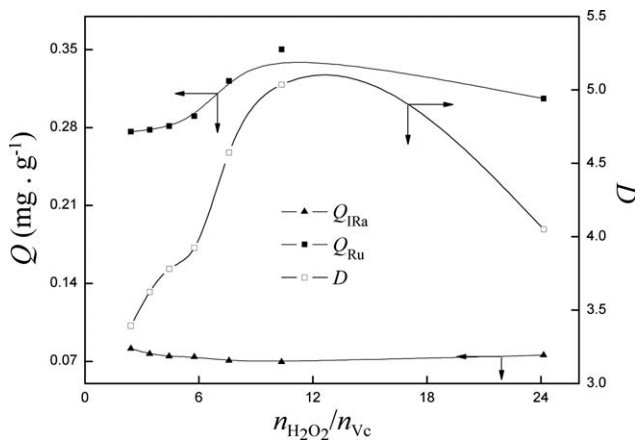

Figure 12 Influence of $n_{H_2O_2}/n_{Vc}$ on the adsorption performance of MIP (T = 45°C; other conditions were the same as Fig. 11 but $n_{H_2O_2}$ and n_{Vc}, $V_{H_2O_2} \neq V_{Vc}$).

acid using Rutin as template. Thereafter, adsorption capacity and separation degree were selected as optimization objective, and the effects of monomers, crosslinker, initiators, polymerization time, and temperature on adsorption selectivity of the prepared MIP were investigated and optimized. The optimum conditions obtained were the molar ratios of Rutin, acrylic acid, NMBA, and hydrogen peroxide to AM were 0.033, 128, 35, and 0.074, hydrogen peroxide to L-ascorbic acid was 10.3, and the polymerization time and temperature were 30 h and 45°C, respectively. MIP prepared at optimum conditions presented favorable adsorption of Ru with a maximal separation degree of 5.0. The obtained MIP with high affinity and excellent stereo-selectivity toward Ru may offer a novel method for the enrichment and extraction of flavonoids in Chinese medicinal herb.

References

1. Komiyama, M.; Takeuchi, T.; Mukawa, T.; Asanuma, H. In Applications of Molecularly Imprinted Polymers; Komiyama, M., Ed.; Federal Republic of Germany Press, Weinheim; p 75–113.
2. Song, X. L.; Li, J. H.; Wang, J. T.; Chen, L. X. Talanta 2009, 80, 694.
3. Itagaki, S.; Oikawa, S.; Ogura, J.; Kobayashi, M.; Hirano, T.; Iseki, K. Food Chem 2010, 118, 426.
4. Afanas'eva, I. B.; Ostrakhovitch, E. A.; Mikhal'chik, E. V.; Ibragimova, G. A.; Korkina, L. G. Biochem Pharmacol 2001, 61, 677.
5. Birt, D. F.; Hendrich, S.; Wang, W. Pharmacol Ther 2001, 90, 157.
6. Xie, J. C.; Zhu, L. L.; Luo, H. P.; Zhou, L.; Li, C. X.; Xu, X. J. J Chromatogr A 2001, 934, 1.
7. Xie, J. C.; Chen, L. R.; Li, C. X.; Xu, X. J. J Chromatogr B 2003, 788, 233.
8. Weiss, R.; Molinelli, A.; Jakusch, M.; Mizaikoff, B. Bioseparation 2002, 10, 379.
9. Xia, Y. Q.; Guo, T. Y.; Song, M. D.; Zhang, B. H.; Zhang, B. L. React Funct Polym 2006, 66, 1734.
10. O'Mahony, J.; Molinelli, A.; Nolan, K.; Smyth, M. R.; Mizaikoff, B. Biosens Bioelectron 2006, 21, 1383.
11. Suárez-Rodríguez, J. L.; Díaz-García, M. E. Biosens Bioelectron 2001, 16, 955.
12. Baggiani, C.; Anfossi, L.; Giovannoli, C.; Tozzi, C. Talanta 2004, 62, 1029.
13. Okutucu, B.; Telefoncu, A. Talanta 2008, 76, 1153.
14. Yu, C.; Mosbach, K. J Chromatogr A 2000, 888, 63.
15. Spivak, D. A. Adv Drug Deliv Rev 2005, 57, 1779.
16. Askari, F.; Nafisi, B.; Omidian, H.; Hashem, S. A. J Appl Polym Sci 1993, 50, 1851.
17. Yan, R. X. In Polyacrylamide; Acrylic Acid and Methacrylic Acid Polymer; Sang, E. D.; Yan, R. X., Eds.; Chemical Industry Press: Beijing, 2001; p 171–192.
18. Wang, B. N.; Song, N. Z. Chin J Anal Chem 1988, 16, 402.
19. Chen, J.; Park, H.; Park, K. J Biomed Mater Res 1999, 44, 53.
20. Chen, Z. B.; Liu, M. Z.; Qi, X. H.; Liu, Z. Polym Eng Sci 2007, 47, 728.
21. Cao, B. Q.; Pan, Y.; Zhao, J. J.; Huang, Q. B. Mod Sci Instrum 2006, 6, 32.
22. Nassar, A. F.; Lucas, S. V.; Hoffland, L. D. Anal Chem 1999, 71, 1285.
23. Chen, Z. B.; Liu, M. Z.; Ma, S. M. React Funct Polym 2005, 62, 85.
24. Lu, Y.; Li, C. X.; Wang, X. D.; Sun, P. C.; Xing, X. H. J Chromatogr B 2004, 804, 53.
25. Andersson, H. S.; Karlsson, J. G.; Piletsky, S. A.; Koch-Schmidt, A. C.; Mosbach, K.; Nicholls, I. A. J Chromatogr A 1999, 848, 39.
26. Vaughan, A. D.; Sizemore, S. P.; Byrne, M. E. Polymer 2007, 48, 74.